Journal of Current Science and Technology, May-August 2021 Vol. 11 No. 2, pp. 197-207
ISSN 2630-0656 (Online)

Cite this article: Sukkasem, C., Sasivimolkul, S., Suvarnaphaet, P., & Pechprasarn, S. (2021, May). Analysis of optical detection of ultrasound using PDMS thin film. *Journal of Current Science and Technology, 11*(2), 197-207. DOI:

Journal of Current Science and Technology

Journal homepage: https://jcst.rsu.ac.th

Analysis of optical detection of ultrasound using PDMS thin film

Chayanisa Sukkasem, Suvicha Sasivimolkul, Phitsini Suvarnaphaet, and Suejit Pechprasarn*

College of Biomedical Engineering, Rangsit University, Patumthani 12000, Thailand

*Corresponding author; E-mail: suejit.p@rsu.ac.th

Received 2 February 2021; Revised 17 April 2021; Accepted 27 April 2021;
Published online 27 May 2021

Abstract

Medical diagnosis and treatments via ultrasound imaging have been challenged to developed using optical detection for sensing signals. The original technique employs a piezoelectric transducer to convert the mechanical energy to electrical energy during creating and sensing the ultrasound signal. However, this technique has some limitations in sensitivity, detection bandwidth, and temperature sensitivity. Herein, we report the simulation results of the optical detection of ultrasonic waves using elastic thin-film material made of polydimethylsiloxane (PDMS). The thickness in the micro-scale of the uniform layer of PDMS at 20 μm thick was observed at the 2 MHz of ultrasonic frequency, showing the PDMS displacement changed linearly by 4.6×10^{-13} m·Pa^{-1}. The response can be detected using the optoacoustic technique with the light at 685 nm wavelength. As the PDMS thickness changed, the responses of light shifted in reflectance and phases, reported the sensitivities of 5.6×10^{-7} Pa^{-1} and 1×10^{-4} rad·Pa^{-1}, respectively. Compared with the traditional detections, the PDMS optical detection using the phase shift achieved much higher sensitivity about 30 times while the detection using the reflectance shift found lower sensitivity 5 times. Nevertheless, the microscale optical sensor's advantage in this work could be an alternative technique because its implementation can be fabricated simpler than traditional sensors and does not require complicated processes.

Keywords**:** *optical detection; optical sensor; optoacoustic technique; PDMS; ultrasound detection; ultrasonic wave.*

1. Introduction

An ultrasonic wave refers to a sound wave with a frequency above 20 kHz (Gallo, Ferrara, & Naviglio, 2018). This technology has been utilized in many applications, such as studying cellular mechanism in biotechnology (Sinisterra, 1992), analyzing and providing the quality of food product in the food industry (Bhargava, Mor, Kumar, & Sharanagat, 2021; Chemat, & Khan, 2011; Gallo et al., 2018) and especially in medicine. Nowadays, ultrasound becomes an essential technology for diagnosing and treatment. In the diagnosis, ultrasound can generate an image of organs or soft tissues by interacting between the ultrasonic wave and the body structure (Carovac, Smajlovic, & Junuzovic, 2011; Coatney, 2001). In the treatment, high- intensity focused ultrasound (HIFU) can remove the human body's tumor due to thermal effect (Hsiao, Kuo, Tsai, Chou, & Yeh, 2016).

Piezoelectric transducers play a significant role in ultrasound detection technology. The piezoelectric effect detect ultrasound by transforming mechanical energy into electrical energy (Manbachi & Cobbold, 2011). The piezoelectric transducer has limited sensitivity and detection bandwidth. There is a tradeoff between ultrasonic detection bandwidth and sensitivity (Dong, Sun, & Zhang, 2017). To design the transducer to operate at a high-frequency regime, precise control of piezoelectric material is crucial. Besides piezoelectric transducers, one of the most challenging aspects is to use the light to detect ultrasound, so-called an optoacoustic technique or

an optical sensor that provides high sensitivity in detection. Optical techniques have been developed for ultrasonic detection, such as a microring resonator (Maxwell et al., 2008) and Fabry-Perot (FP) interferometer (Beard, Perennes, & Mills, 1999). Both techniques require complicated and advance instruments for structure fabrication. Lately, Learkthanakhachon, Pechprasarn and Somekh (2018) presented that polydimethylsiloxane (PDMS) thin-film can be investigated in optical ultrasonic detection with high sensitivity (Learkthanakhachon, Pechprasarn, & Somekh, 2018).

In this work, we have proposed the simulation results of elastic thin-film of PDMS material under ultrasonic wave and investigating response of the PDMS thin film using the optical detection platform. The simulation employed elastic characteristics of micro-scale PDMS thin film under the ultrasonic wave with the frequency of 2 MHz and amplitude of 0 – 4300 kPa loaded on the top of the optical sensor platform. The light can observe the response of PDMS thin film at 685 nm wavelength, and its properties change in terms of reflectance and phase. In this work, the PDMS thin film showed the sensitivities response changed due to the variation of thickness linearly, which is based on optoacoustic technology.

2. Objectives

The objective of this work was to investigate the simulation behaviors of the PDMS thin film influenced by ultrasound compression and the responses using the optical detection platform based on the PDMS thin film to find out the sensing performance in terms of reflectance and phase shifts. Also, to compare the sensitivities of our ultrasound detection with traditional optical techniques.

3. Materials and methods

Mathematical model and calculations studied the theoretical analysis of ultrasound detection using the elastic PDMS thin film. The simulation processes consisted of two parts, including 1) the simulation of the characteristic of the PDMS thin film under compression by ultrasonic wave with various thicknesses, and 2) the simulation of sensing performance of the ultrasound detection based on the optical platform using PDMS thin film.

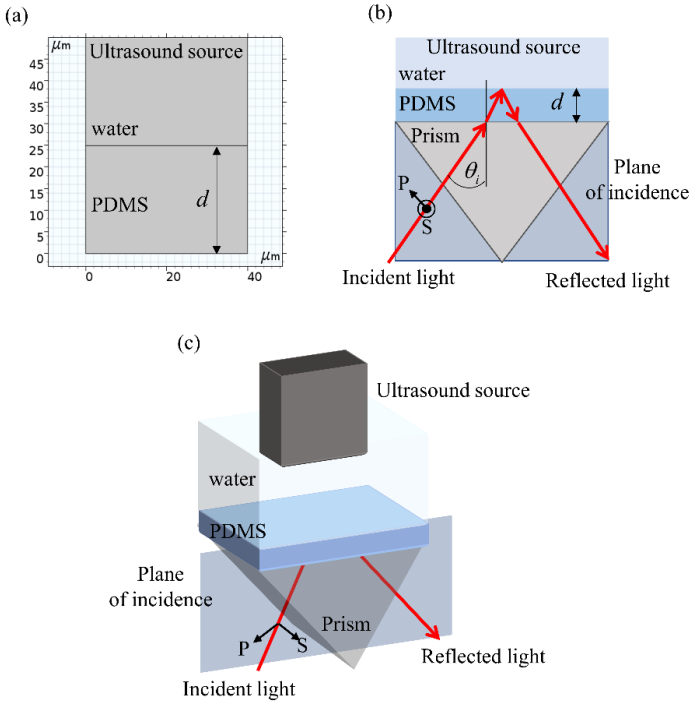

Figure 1 (a) Schematic diagram of PDMS thin film under an ultrasonic wave at 2 MHz frequency, (b) an optical detection platform using PDMS thin film, and (c) 3-dimensional (3D) schematic setup of the optical ultrasound detection.

3.1 Modeling setup for ultrasound compression

As seen in Figure 1a, two layers consisting of the micro-scale elastic thin-film made of PDMS are used as a sensitive-layered material in the schematic model. Water at a temperature of 20°C is used as a medium layer to apply the ultrasonic wave. Assuming the effect of the thermal change is neglected. This model was simulated using the finite element method (FEM) in the COMSOL Multiphysics 5.2a program. The ultrasonic plane wave was generated using an ultrasound probe with a constant frequency of 2 MHz on the top of the water layer, where the water is the medium for the travelling wave. Hence the ultrasonic wave was transferred through the PDMS layer. The behaviors of the PDMS thin-film layer under the ultrasound compression was investigated because of an acoustic – solid interaction in the frequency domain. This model can be employed to study the PDMS structural deformation, including the displacement change and stress in material under acoustic pressure conditions. The traveling speed of the ultrasound in water was applied at 1484 m/s (Chávez, Sosa, & Tsumura, 1985). The mechanical properties of the PDMS material were referenced from the experimental results of the Learkthanakhachon et al. (2018). The ultrasonic wave frequency was applied at 2 MHz, Young's modulus of the PDMS material was reported 123.4 MPa (Learkthanakhachon et al., 2018), and the Poisson's ratio was given by 0.43 (Dogru, Aksoy, Bayraktar, & Alaca, 2018). The difference in ultrasonic wave frequencies loaded was reported influence to the PDMS material in mechanical responses due to the difference of Young's modulus (Pottier, Ducouret, Frétigny, Lequeux, & Talini, 2011). This simulation was set the mesh size of 15–200 nm. The study investigates the displacement changes in the PDMS layer under ultrasound compression by varying the PDMS thin-film thickness (d) and using different acoustic pressure (P).

3.2 Modeling setup for optical detection using PDMS thin film

To carry out the response of PDMS layer under ultrasound compression, the PDMS thin film was modelled as the sensitive layer on the optical detection platform based on Fresnel's equation (Zhang & Hoshino, 2019) where the mathematical simulation was operated using MATLAB 2019. Figures 1b and 1c illustrated the optical detection platform comprising layers of PDMS thin film, water medium, and ultrasound source placed on top of the glass prism. Recently, the coherent light source with 685 nm wavelength has been studied the sensitivity performances of optical ultrasound detection with the shearing interferometer technique (Learkthanakhachon et al., 2018). Therefore, the light at 685 nm wavelength was chosen to compare our platform with the previous work. The incident light refers to the light at the interface between the glass prism, and the PDMS thin film is with the incident angle of θ_i. Optically, the light refers to an electromagnetic wave carrying P-polarization parallel to the plane of incidence, whereas the S-polarization perpendicular to the plane of incidence. This calculation based on Fresnel's equation had provided optical reflectance and phase responses of the PDMS thin film depending on the thickness changes when the ultrasonic wave loaded. Figure 1c showed the 3D view setup when the ultrasound probe placed on top and the reflected light observed by a photodetector. Fresnel's equation is a well-known equation usually studying the reflectance and transmittance effects of an electromagnetic wave when the light is incident on different medium, and the refractive index (n) of the medium is different (Yevick, Rolland, Bardyszewski, & Hermansson, 1990). Figure 1b shows a diagram of the simulation model where the parameters and values are shown in Table 1.

Table 1 shows the parameters used in simulations

Parameters	Values	References
Simulation of the PDMS thin film under ultrasound compression		
Young's modulus of PDMS	123.4 MPa	Learkthanakhachon et al., 2018
Poisson's ratio of PDMS	0.43	Dogru et al., 2018
Temperature of medium	20°C	Chávez et al., 1985
Speed of ultrasound in the medium	1484 m/s	Chávez et al., 1985
Simulation of the optical detection using PDMS		
Wavelength of light	685 nm	Learkthanakhachon et al., 2018
n_{prism}	1.5200	Nakamura Tsutsumi, Juni, & Fujii, 2005
n_{pdms}	1.4278	Schneider, Draheim, Kamberger, & Wallrabe, 2009
n_{water}	1.3300	Hale & Querry, 1973

The ultrasound detection performance using PDMS thin film can be quantified by sensitivity defined as expressed in equations (1) and (2),

$$\text{Sensitivity for reflectance} = \frac{dR}{dP} \quad (1)$$

and

$$\text{Sensitivity for phase detection} = \frac{d\phi}{dP}, \quad (2)$$

where R is the reflectance. ϕ is the phase response in rad, and P is the incident acoustic pressure in Pa.

4. Results and discussion

The simulation results of PDMS thin film compressed under the ultrasound conditions using the constant frequency of 2 MHz and the amplitude of 500 kPa. Figure 2 illustrated that the PDMS thin film with 20 μm thick was compressed at which the ultrasound incident perpendicularly to the surface. The color bar showed the displacement strength. As seen in Figure 2a and 2b, the surface of PDMS was uniformly deflated by 23 nm. Figure 2c shows the effect of PDMS thin film thickness on compressibility. The maximum compressibility took place for the thickness of 20 μm PDMS layer. The thinner PDMS, the lower compressibility was comparing to thicker PDMS thin film. Not only these phenomena occurred in the case of PDMS thin film under the ultrasound pressure loaded, the literature also reported that other mechanical properties, such as residual stress and stiffness, depended on the structure size and thickness (Abazari, Safavi, Rezazadeh, & Villanueva, 2015). It was found that the PDMS thin film with different thickness between 15 μm and 50 μm provided good compressibility under the ultrasound at 2 MHz frequency. Using 20-μm PDMS thin film, the compressed displacement was 4.6×10^{-13} m·Pa^{-1} which well agreed with the experimental results reported by Learkthanakhachon et al. (2018).

Figure 2d showed the compressed displacement of PDMS thin film under 2 MHz with different pressures or amplitudes of wave ranging from 0 to 1000 kPa. For several thicknesses of 5 μm, 20 μm, and 60 μm, the rates of displacement change were investigated as the slopes and found 2.4×10^{-13} m·Pa^{-1}, 4.6×10^{-13} m·Pa^{-1}, and 3.8×10^{-13} m·Pa^{-1}, respectively. The effect of acoustic pressure on PDMS thin film compressibility showed linear behaviors in all conditions, and the PDMS compressibility agreed with the results in Figure 2c. The relationship of the ultrasonic amplitude and the compressibility based on displacement changes were agreed with Hook's law, as shown in equation (3).

$$\sigma = E \cdot \epsilon \quad (3)$$

where σ is the tensile stress calculated from the applied force (F) and cross-sectional area of the material, thus $\sigma = \frac{F}{A}$. E is Young's modulus of the material. ϵ is the strain calculated by the thickness change (Δd) of material and its initial length (d_0), $\epsilon = \frac{\Delta d}{d_0}$.

The ultrasonic wave can induce two types of change in PDMS thin film, i.e. the thickness and the material stress. The stress in the PDMS material was influent on the reflective index of the material. For the elastic material, the ultrasonic pressure of 1 MPa can change the refractive index of 1×10^{-4} RIU (Chao, Ashkenazi, Huang, Donnell, & Guo, 2007), which was relatively small and neglected in this study. Note that the RIU unit is Refractive Units Index usually used in optical biosensing.

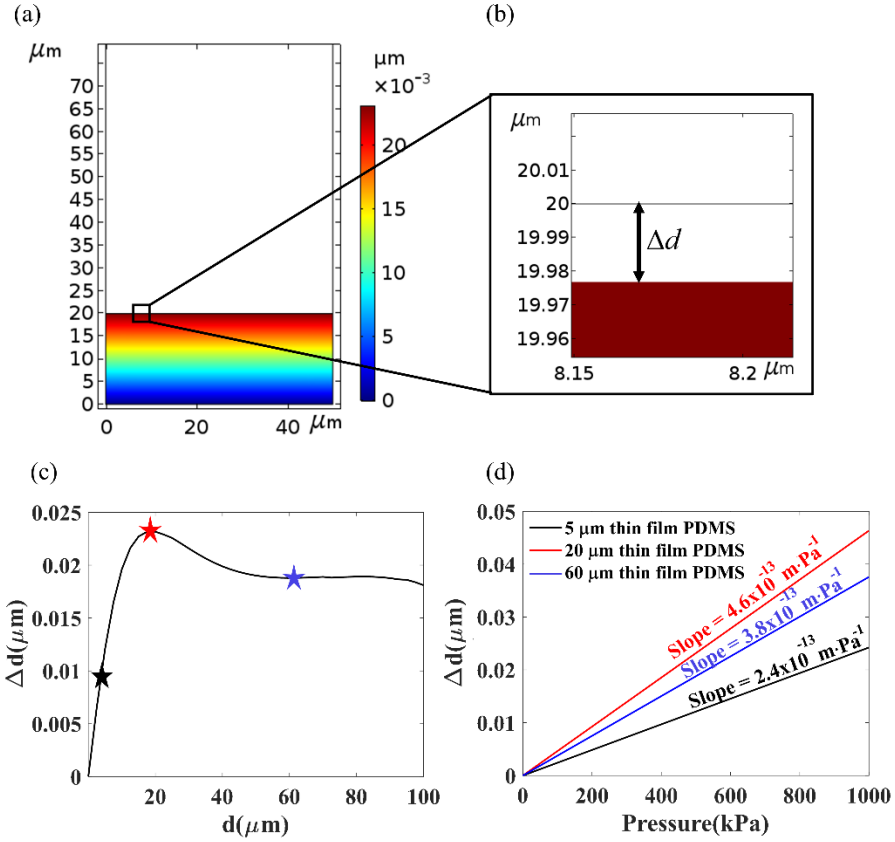

Figure 2 (a) PDMS thin film with 20 μm thick and (b) the displacement changes at the surface of 20-μm PDMS thin film by 23 nm under uniform compression of ultrasound with a frequency of 2 MHz and amplitude of 500 kPa. A color bar denotes the displacement of PDMS thin film. (c) The PDMS thin film thickness change (Δd) with varying PDMS thin film thickness (d) ranging from 0-100 μm and (d) the linear relationship of ultrasound pressure and the PDMS film displacement change for different thickness in (c), i.e. 5 μm (black), 20 μm (red) and 60 μm (blue) and their rates of change.

From the optical simulation, the critical parameters in this optical system were the critical angle, θ_c, the angle of incidence, which produced the angle of refraction of the light at 90°. It was considered that if the incident angle was lower than the critical angle, the incident light transmitted through the incident boundary, otherwise reflected. If the incident angle was higher than the critical angle, all of the incident light only reflected, referring to light cannot transmit through the boundary. The critical angle can be calculated using Snell's law (Li & Mueller, 2005), as shown in equation (4);

$$n_i \sin\theta_i = n_r \sin\theta_r , \qquad (4)$$

where
n_i is the refractive index of the first medium,
n_r is the refractive index of the second medium,
θ_i is the incident angle at the two-medium boundary, and
θ_t is the angle of refraction of transmitted light.

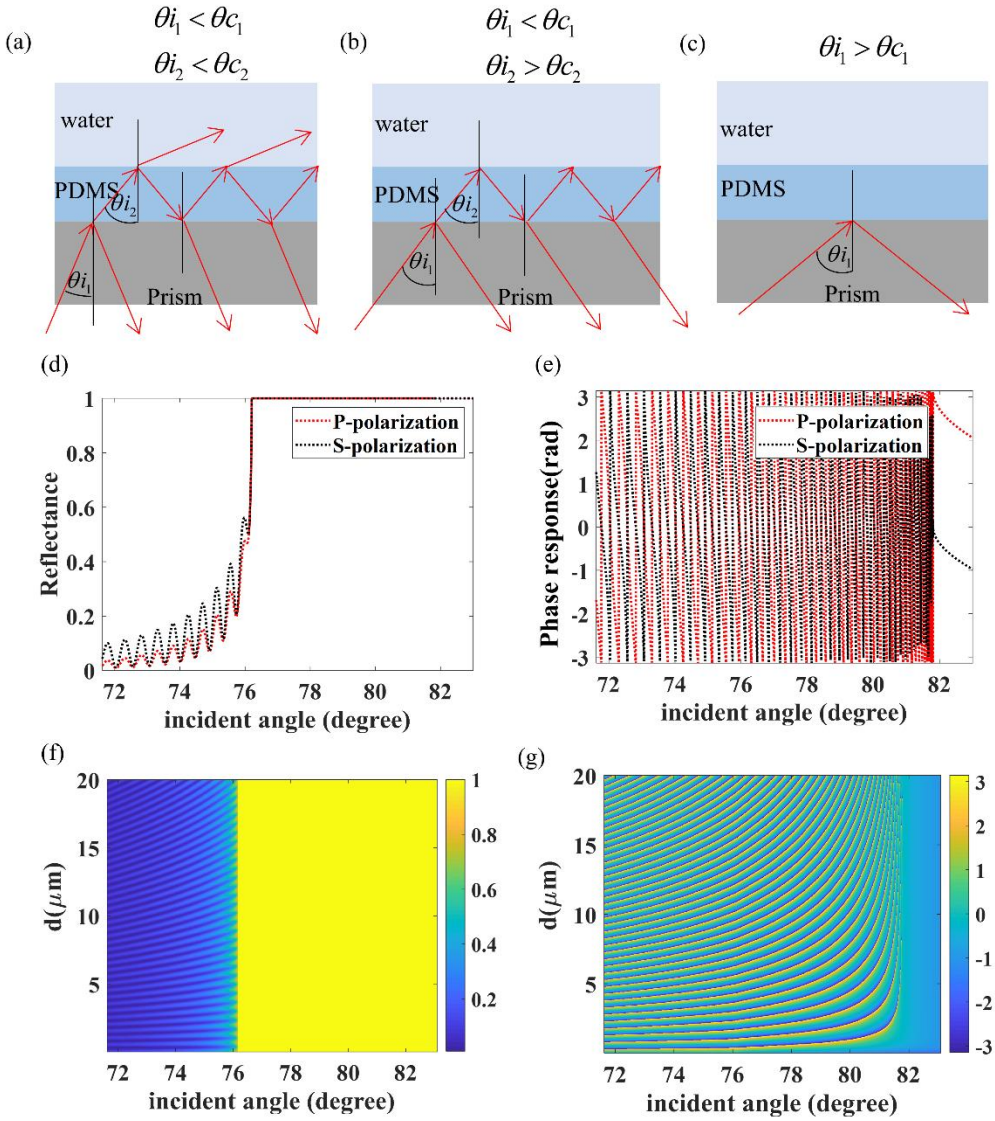

Figure 3 shows (a) diagram of optical response when the incident angle less than the critical angles, θ_c, of two PDMS boundaries, (b) diagram of optical response when the incident angle less than the critical angle in glass-PDMS boundary degree of incident angle is more than critical angle in PDMS-water boundary, (c) diagram of optical response when the incident angle is more than critical angle in glass-PDMS boundary, (d) reflectance of P-polarization and S-polarization with 20 □m thick PDMS, (e) phase response in rad of P-polarization and S-polarization with 20 □m thick PDMS (f) reflectance as a function of PDMS thin film thickness and the incident angle for the S- polarization, and (g) phase response in rad as a function of PDMS thin film thickness and the incident angle for the S- polarization.

In the optical simulation, the incident light traveled through the two boundaries of PDMS, i.e. the glass-PDMS boundary and the PDMS-water boundary, as shown in Figure 1b and 1c. These two boundaries have different critical angles. The critical angle of the glass-PDMS boundary was found 81.8°, and the critical angle of the PDMS-water boundary was 76.2°. The angle of incident light at the glass-PDMS boundary was less than at the PDMS-water boundary based on the angle of refraction of Snell's law. Three effects were observed in this system. First, both incident angles at the boundaries were less than the critical angle, as shown in Figure 3a. This effect provided transmission and reflection at both boundaries. The reflectance would be low because some of the incident light transmitted through the water. The reflectance responses showed in Figures 3d and 3f when the incident angles were less than 76.2°. Since the incident light illuminating the optical

system was coherent. The reflected light beams from the two interfaces caused the interference and formed a resonant cavity. The phase responses of the interference were shown in Figures 3e and 3g. Second, the incident angle at the PDMS-water boundary was more than the PDMS glass interface's critical angle, as shown in Figure 3b. The incident light at the glass-PDMS boundary would be transmitted and reflected. The incident light at the PDMS-water boundary would be reflected and travel through the glass-PDMS boundary. This effect can provide a total internal reflection effect in the PDMS layer. There is no light energy going out of this system through the transmission. The reflectance from this effect equal to 1, as shown in Figures 3d and 3f. However, the reflected light of the two boundaries can also interfere with each other. The result of the phase response of interference was shown in Figures 3e and 3g. Last effect, the angle of incident light at the glass-PDMS boundary was larger than the PDMS-glass interface critical angle of 81.8°, as shown in Figure 3c. All incident light was reflected at the glass-PDMS boundary. The incident light cannot transmit to the PDMS layer. This effect cannot provide the interference, as shown in Figures 3e and 3g, and the reflectance of this effect equal to 1, as shown in Figures 3d and 3f.

Figures 3d and 3e showed the optical simulation results of reflectance and phase response for the P-polarization and the S-polarization for the ultrasonic detection using PDMS thin film. The PDMS thin film with 20 □m thickness at different incident angles was investigated in this study. Figure 3d shows that the S-polarization reflectance response was better than the P-polarization case. The P-polarization provided a perfect transmission at the PDMS boundary when the incident angle equals Brewster's angle. For the phase response, the S-polarization and the P-polarization were antiphase with each other. The reflectance of the intensity pattern for both polarizations was similar, as shown in Figure 3e. Herein, the results of the P-polarization were omitted to save the space of this manuscript.

Figures 3f and 3g illustrated the reflectance and phase response for incident angles and PDMS thin film thickness, d, for the S-polarization. The result showed that when the thin-film thickness changes, the phase of reflected light from the PDMS-water boundary was also changed due to the difference in the optical path length.

There are 2 methods for investigating this effect in ultrasonic detection, reflectance measurement and phase detection. The ultrasonic detection can be realized by measuring the reflectance difference when the incident angle was less than the PDMS-water boundary's critical angle of 76.2°. This technique detected ultrasonic waves by comparing the intensity of reflected light with and without ultrasonic loading. For phase detection, this method required an interferometric system. An interferometer is very sensitive to the environment, and it usually requires a vibration isolation system. The phase measurement method can be employed when the incident angle was less than the critical angle of the glass-PDMS boundary of 81.8°.

Figure 4a showed the reflectance result with varying PDMS thickness and two incident angles at the glass-PDMS boundary of 72° and 76°. The figure expressed that the different incident angles can give a different reflectance response due to the change in PDMS thickness, □R/□d. The higher incident angle can provide a higher sensitivity than a lower incident angle. The incident angle of 76° responded to the reflectance due to the change of PDMS thickness of 1.22×10^{6} m^{-1}, and the incident angle of 72° responded to the PDMS thickness of 6.10×10^{5} m^{-1}. Moreover, the result showed that the thickness of PDMS thin film before ultrasonic wave loading did not affect the response. The pattern of reflectance response did not change when the PDMS thin film thickness changed.

The change in reflectance was due to PDMS thin film thickness changes modulated by the incident ultrasonic waves. Figure 4b showed how the optical system reflectance and phase response illuminated by the ultrasonic wave with a frequency of 2 MHz and amplitude of 0 – 4300 kPa. The reflectance response of the system was non-linear. The reflectance measurement has the highest sensitivity, 5.62×10^{-7} Pa^{-1}, calculated by equation (4), which agreed with the experiment reported in Learkthanakhachon et al. (2018) results. In the phase response, Figure 4c showed a comparison between phase responses of two incident angles of 0° and 76° with the PDMS thin film thickness and the ultrasonic pressure. Lower incident angles provided better sensitivity to ultrasonic waves than that of the traditional methods exceeding 30 times. The highest sensitivity of phase-detection occurs at the incident angle of 0° with the sensitivity of 1×10^{-4} rad□Pa^{-1}. For the incident angle of 0 degrees, the

light that travels in the shortest light path comparing to another incident angle provides a well-defined phase shift, as shown in Figure 4c. Finally, the phase-detection presented better sensitivity on sensing ultrasound than reflectance detection; therefore this work could promise as an optical interferometer.

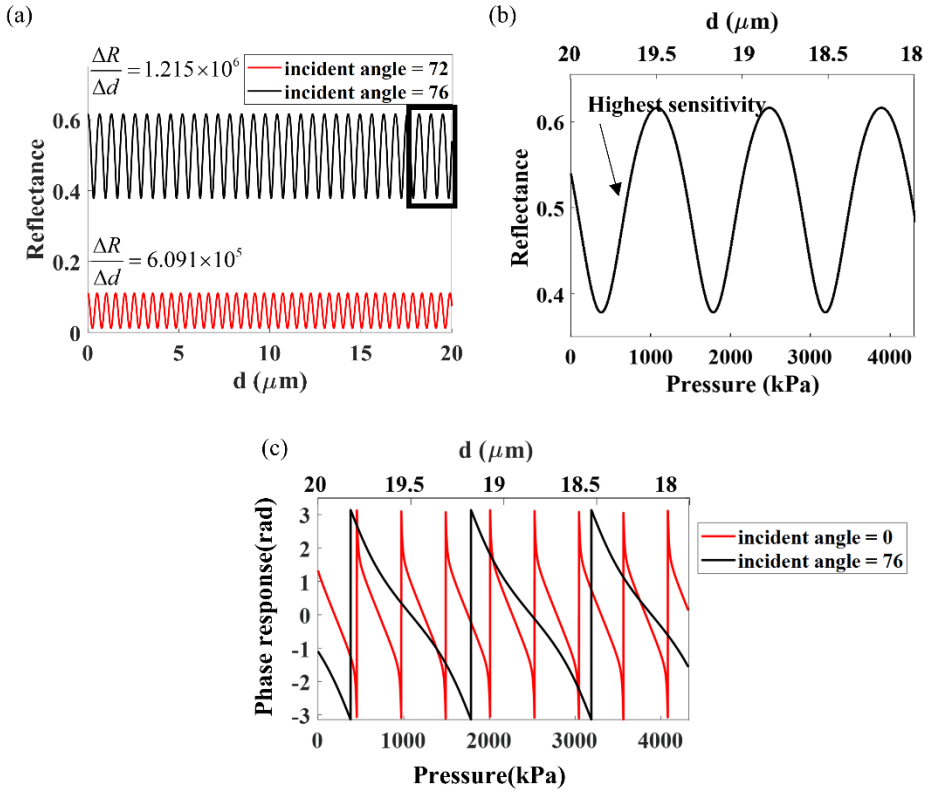

Figure 4 (a) Reflectance of different PDMS thicknesses illuminated by the incident angles of 72° and 76°, (b) reflectance responses for the incident angle of 76° with the incident ultrasonic pressure of 0 to 4300 kPa, and (c) phase response in rad for the incident angles of 0° and 76° with the incident ultrasonic pressure of 0 to 4300 kPa.

5. Conclusions

This study has investigated how the uniform PDMS thin film is employed for optical detection of ultrasonic waves through the modelling and computer simulation. The PDMS layer can be compressed by the incident ultrasonic waves leading to the change in the PDMS film optical path length, which can be optically measured using an interferometer. The effect of the ultrasonic loading on the PDMS can be observed in changes in the optical reflectance and the reflected light phase response. Both of these responses can be realized and detected in different experimental configurations. For the phase response, the PDMS film can provide higher sensitivity of $1x10^{-4}$ rad·Pa^{-1}. However, the phase-detection does require an interferometer system to measure the relative phase difference between the unloading and loading of ultrasonic waves. For the reflectance measurement, the ultrasonic wave measurement can be detected by measure the change in intensity of reflected light between unloading and loading of the ultrasonic wave. The intensity measurement does not require an anti-vibration system. The reflectance measurement can provide sensitivity in ultrasonic detection of $5.6x10^{-7}$ Pa^{-1}. Compared to traditionally optical-ultrasonic detection techniques, such as a ring resonator (Ashkenazi, Chao, Guo, & O'Donnell, 2004), an FP sensor (Beard et al., 1999), and a surface plasmon resonance (SPR) sensor (Sangworasil et al., 2016) have been reported the sensitivities of $3.0x10^{-6}$ Pa^{-1}, $2.1x10^{-6}$ μW·Pa^{-1}, and $1.4x10^{-10}$ RIU·Pa^{-1}, respectively. In our method, even the PDMS thin film platform is observed only for the reflectance detection giving five times lower sensitivity than the other traditional optical

detection, but it is observed 4,000 times higher than the sensitivity of the SPR technique. For phase detection, it provides the highest sensitivity compared to the other methods. For typical medical ultrasound imaging, the sensitivity requirement is 14–650 kPa (Couture, Fink, & Tanter, 2012). However, higher sensitivity in ultrasonic detection can be employed in the photoacoustic imaging (PI) technique. This technique requires high sensitivity due to the low magnitude of pressure in the PI system, high-frequency sources, and the ultrasound's attenuation. For example, to image the blood vessel by detecting requires the ultrasonic pressure of 3–6 kPa (X. Zhang et al., 2019). Also, for the photoacoustic computed tomography (PACT), this technique is employed to study the function of the small and *in vivo* sample, such as mouse's brain (Nasiriavanaki et al., 2014; Yao et al., 2013). For the comparison in complexity, the phase detection requires a sophisticated interferometer to measure the phase shift response, whereas the reflectance response techniques, such as the PDMS-based reflectance measurement, SPR sensor, and FP-based sensor, do not require a complex system. The ultrasonic detection-based piezoelectric sensor requires an electrical circuit and isolation system to control the vibration of the material. The additional advantage of using PDMS thin film is that it is cost-effective based on a less demanding fabrication process than piezoelectric materials. The PDMS layer's fabrication is not complicated and does not require a sophisticated protocol and an advanced instrument. The conventional spin coating process can be employed to fabricate the uniformly PDMS thin film (Thangawng, Ruoff, Swartz, & Glucksberg, 2007), including PDMS has low manufacturing costs (Mata, Fleischman, & Roy, 2006). The uniformity of the PDMS thin film can be achieved in a wide range of thickness ranging from 2.5 μm to 40 μm (Yan, Zhou, Zhang, Guo, & Guo, 2018), including PDMS, has low manufacturing costs (Mata et al., 2006). However, PDMS material has a practical issue. The thermal change can affect the expansion of the PDMS with an expansion coefficient of 300 nm/°C; therefore, the temperature should be controlled by a closed-loop temperature control unit (Lowndes & Hallett, 1986).

6. Acknowledgements

The Research Institute of Rangsit University funded this work. CS and SS also thank Biophysics and Medical Optic laboratory, College of Biomedical Engineering, to support facilities during research.

7. References

Abazari, A., Safavi, S. M., Rezazadeh, G., & Villanueva, L. G. (2015). Modelling the size effects on mechanical properties of micro/nano structures. *Sensors*, *15*(11), 28543-28562. DOI: 10.3390/s151128543

Ashkenazi, S., Chao, C.-Y., Guo, L., & O'Donnell, M. (2004). Ultrasound detection using polymer microring optical resonator. *Applied Physics Letters*, *85*(22): 5418-5420. DOI: 10.1063/1.1829775

Beard, P. C., Perennes, F., & Mills, T. N. (1999). Transduction mechanisms of the Fabry-Perot polymer film sensing concept for wideband ultrasound detection. *IEEE Transactions on Ultrasonics, Ferroelectrics, and Frequency Control*, *46*(6), 1575-1582. DOI: 10.1109/58.808883

Bhargava, N., Mor, R. S., Kumar, K., & Sharanagat, V. S. (2021). Advances in application of ultrasound in food processing: A review. *Ultrasonics Sonochemistry*, *70*, 105293. DOI: https://doi.org/10.1016/j.ultsonch.2020.105293

Carovac, A., Smajlovic, F., & Junuzovic, D. (2011). Application of ultrasound in medicine. Acta informatica medica : AIM : journal of the Society for Medical Informatics of Bosnia & Herzegovina : casopis *Drustva za medicinsku informatiku BiH*, *19*(3), 168-171. DOI: 10.5455/aim.2011.19.168-171

Chávez, M., Sosa, V., & Tsumura, R. (1985). Speed of sound in saturated pure water. *Journal of The Acoustical Society of America - J ACOUST SOC AMER*, *77*(2), 420-423. DOI: 10.1121/1.391861

Chao, C., Ashkenazi, S., Huang, S., Donnell, M. O., & Guo, L. J. (2007). High-frequency ultrasound sensors using polymer microring resonators. *IEEE Transactions on Ultrasonics, Ferroelectrics, and Frequency Control*, *54*(5), 957-965. DOI: 10.1109/TUFFC.2007.341

Chemat, F., & Khan, M. K. (2011). Applications of ultrasound in food technology: processing, preservation and

extraction. *Ultrasonics sonochemistry*, *18*(4), 813-835. DOI: https://doi.org/10.1016/j.ultsonch.2010.11.023

Coatney, R. W. (2001). Ultrasound imaging: principles and applications in rodent research. *ILAR journal*, *42*(3), 233-247. DOI: 10.1093/ilar.42.3.233

Couture, O., Fink, M., & Tanter, M. (2012). Ultrasound contrast plane wave imaging. *IEEE Transactions on Ultrasonics, Ferroelectrics, and Frequency Control*, *59*(12), 2676-2683. DOI: 10.1109/tuffc.2012.2508

Dogru, S., Aksoy, B., Bayraktar, H., & Alaca, B. E. (2018). Poisson's ratio of PDMS thin films. *Polymer Testing*, *69*, 375-384. DOI: https://doi.org/10.1016/j.polymertesting.2018.05.044

Dong, B., Sun, C., & Zhang, H. F. (2017). Optical detection of ultrasound in photoacoustic imaging. *IEEE transactions on bio-medical engineering*, *64*(1), 4-15. DOI: 10.1109/TBME.2016.2605451

Gallo, M., Ferrara, L., & Naviglio, D. (2018). Application of ultrasound in food science and technology: A perspective. *Foods (Basel, Switzerland)*, *7*(10), 164. DOI: 10.3390/foods7100164

Hale, G. M., & Querry, M. R. (1973). Optical Constants of Water in the 200-nm to 200-microm Wavelength Region. *Applied Optics*, *12*(3), 555-563. DOI: 10.1364/ao.12.000555

Hsiao, Y. H., Kuo, S. J., Tsai, H. D., Chou, M. C., & Yeh, G. P. (2016). Clinical application of high-intensity focused ultrasound in cancer therapy. *Journal of cancer*, *7*(3), 225. DOI: 10.7150/jca.13906

Learkthanakhachon, S., Pechprasarn, S., & Somekh, M. G. (2018). Optical detection of ultrasound by lateral shearing interference of a transparent PDMS thin film. *Optics Letters*, *43*(23), 5797. DOI: 10.1364/OL.43.005797

Li, S., & Mueller, K. (2005). Accelerated, high-quality refraction computations for volume graphics. *Proceedings of the Fourth Eurographics / IEEE VGTC conference on Volume GraphicsJune 2005* Pages 73-81.

Lowndes, R., & Hallett, M. B. (1986). A versatile light microscope heating stage for biological temperatures. *Journal of microscopy*, *142*(3), 371-374. DOI: https://doi.org/10.1111/j.1365-2818.1986.tb04292.x

Manbachi, A., & Cobbold, R. S. C. (2011). Development and application of piezoelectric materials for ultrasound generation and detection. *Ultrasound*, *19*(4), 187-196. DOI: 10.1258/ult.2011.011027

Mata, A., Fleischman, A., & Roy, S. (2006). Characterization of Polydimethylsiloxane (PDMS) Properties for Biomedical Micro/Nanosystems. *Biomedical Microdevices*, *7*(4), 281-293. DOI: 10.1007/s10544-005-6070-2

Maxwell, A., Huang, S.-W., Ling, T., Kim, J.-S., Ashkenazi, S., & Guo, L. J. (2008). Polymer microring resonators for high-frequency ultrasound detection and imaging. *IEEE journal of selected topics in quantum electronics: a publication of the IEEE Lasers and Electro-optics Society*, *14*(1), 191-197. DOI: 10.1109/JSTQE.2007.914047

Nakamura, T., Tsutsumi, N., Juni, N., & Fujii, H. (2005). Thin-film waveguiding mode light extraction in organic electroluminescent device using high refractive index substrate. *Journal of applied physics*, *97*(5), 054505.

Nasiriavanaki, M., Xia, J., Wan, H., Bauer, A. Q., Culver, J. P., & Wang, L. V. (2014). High-resolution DOI: https://doi.org/10.1063/1.1858875photoacoustic tomography of resting-state functional connectivity in the mouse brain. *Proceedings of the National Academy of Sciences*, *111*(1), 21-26. DOI: https://doi.org/10.1073/pnas.1311868111

Pottier, B., Ducouret, G., Frétigny, C., Lequeux, F., & Talini, L. (2011). High bandwidth linear viscoelastic properties of complex fluids from the measurement of their free surface fluctuations. *Soft Matter*, *7*(17), 7843-7850. DOI: 10.1039/C1SM05258F

Sangworasil, M., Pechprasarn, S., Learkthanakhachon, S., Ittipornnuson, K., Suvarnaphaet, P., & Albutt, N. (2016, 7-9 Dec. 2016). Investigation on feasibility of

using surface plasmons resonance (SPR) sensor for ultrasonic detection: A novel optical detection of ultrasonic waves. Paper presented at the *2016 9th Biomedical Engineering International Conference (BMEiCON 2016*). Laung Prabang, Laos 7-9 December 2016.

Schneider, F., Draheim, J., Kamberger, R., & Wallrabe, U. (2009). Process and material properties of polydimethylsiloxane (PDMS) for Optical MEMS. *Sensors and Actuators A: Physical*, *151*(2), 95-99. DOI: https://doi.org/10.1016/j.sna.2009.01.026

Sinisterra, J. V. (1992). Application of ultrasound to biotechnology: an overview. Ultrasonics, 30(3), 180-185. doi:https://doi.org/10.1016/0041-624X(92)90070-3

Thangawng, A. L., Ruoff, R. S., Swartz, M. A., & Glucksberg, M. R. (2007). An ultra-thin PDMS membrane as a bio/micro–nano interface: fabrication and characterization. *Biomedical Microdevices*, *9*(4), 587-595. DOI: 10.1007/s10544-007-9070-6

Yan, Y., Zhou, P., Zhang, S.-X., Guo, X.-G., & Guo, D.-M. (2018). Effect of substrate curvature on thickness distribution of polydimethylsiloxane thin film in spin coating process. *Chinese Physics B*, *27*(6), 068104. DOI: 10.1088/1674-1056/27/6/068104

Yao, J., Xia, J., Maslov, K. I., Nasiriavanaki, M., Tsytsarev, V., Demchenko, A. V., & Wang, L. V. (2013). Noninvasive photoacoustic computed tomography of mouse brain metabolism in vivo. *Neuroimage*, *64*, 257-266. DOI: 10.1016/j.neuroimage.2012.08.054

Yevick, D., Rolland, C., Bardyszewski, W., & Hermansson, B. (1990). Fresnel studies of reflected beams. *IEEE Photonics Technology Letters*, *2*(7), 490-492. DOI: 10.1109/68.56630

Zhang, J. X. J., & Hoshino, K. (2019). Chapter 5 - Optical transducers: Optical molecular sensing and spectroscopy. In J. X. J. Zhang & K. Hoshino (Eds.), Molecular Sensors and Nanodevices (Second Edition) (pp. 231-309): Academic Press. *Principles, Designs and Applications in Biomedical Engineering Micro and Nano Technologies*. DOI: https://doi.org/10.1016/B978-0-12-814862-4.00005-3

Zhang, X., Weng, C., Wu, S., Cai, J., Wu, H., Li, Z., ... & Li, H. (2019). Photoacoustic identification of blood vessel deformation under pressure. *AIP Advances*, *9*(7), 075019. DOI: https://doi.org/10.1063/1.5108852